The ^{40}Ca$(t,p)^{42}$Ca reaction at triton energies near 10 MeV per nucleon

M. B. Becha,* C. O. Blyth, and C. N. Pinder†
School of Physics and Space Research, University of Birmingham, Edgbaston, Birmingham B15 2TT, United Kingdom

N. M. Clarke‡ and R. P. Ward§
School of Physics and Space Research, University of Birmingham, Edgbaston, Birmingham B15 2TT, United Kingdom and Wheatstone Laboratory, King's College London, Strand, London WC2R 2LS, United Kingdom

P. R. Hayes** and K. I. Pearce††
Wheatstone Laboratory, King's College London, Strand, London WC2R 2LS, United Kingdom

D. L. Watson, A. Ghazarian,‡‡ and M. D. Cohler
Department of Physics, University of York, Heslington, York YO1 5DD, United Kingdom

I. J. Thompson
Department of Physics, University of Surrey, Guildford GU2 5XH, United Kingdom

M. A. Nagarajan§§
Science and Engineering Research Council, Daresbury Laboratory, Warrington WA4 4AD, United Kingdom
(Received 16 June 1997)

Two nucleon transfer reactions have been used to probe for correlations in nuclei but there have been doubts about the assumptions made and hence about the success of the analyses. An experimental study of the ^{40}Ca$(t,p)^{42}$Ca reaction at incident triton energies of 10–15 MeV/nucleon was made to determine if the one-step, two-nucleon transfer mechanism was dominant at these energies. Measurements were made with 28, 33, and 37.3 MeV incident energy and particular care was taken to measure absolute differential cross sections for transitions to several residual states in ^{42}Ca. The analysis of all the data used the results of full finite-range calculations and care was taken to calculate all the one-step and two-step reaction channels in a consistent manner starting from a shell-model description of the relevant Ca isotopes with a single, large basis set of single-particle wave functions. Although a complete prediction of the data was not achieved, it is concluded that incident triton energies about 10 MeV/nucleon are still not enough for one-step, two-nucleon transfer to dominate the (t,p) reaction mechanism. Even with a full analysis, it was not possible to reliably extract the reaction amplitudes by fitting the data because of the effects of the discrete potential ambiguity when describing elastic scattering. Hence it is not possible to extract accurate data about two-nucleon correlations in nuclei from (t,p) reactions at these energies. Additionally, some measurements on the ^{8}Ca$(t,p)^{50}$Ca reaction with 37.3 MeV incident energy are presented. Using a similar analysis, calculations predicted the magnitude of the differential cross-section data and the structure of the angular distributions. The J^{π} of the second excited state of ^{49}Ca was shown to be $7/2^{-}$. [S0556-2813(97)05110-8]

PACS number(s): 25.55.Hp, 24.10.Eq, 27.40.+z

*Present address: HMIT Waterloo 2 TDO, 20 Lavington St., London SE1 0NN, United Kingdom.
†Present address: B T Laboratories, Martlesham Heath, Ipswich IP5 7RE, United Kingdom.
‡Present address: School of Physics and Astronomy, University of Birmingham, Edgbaston, Birmingham B15 2TT, United Kingdom.
§Present address: School of Sciences, Staffordshire University, College Road, Stoke-on-Trent ST4 2DE, United Kingdom.
**Present address: Office of Science and Technology, Department of Trade and Industry 84-86 Petty France, London SW1H 9ST, United Kingdom.
††Present address: Magnox Electric plc, Berkeley Technology Centre, Berkeley, Gloucestershire GL13 9PB, United Kingdom.
‡‡Deceased.
§§Present address: Departamento de Física, Atómica, Molecular y Nuclear, Facultad de Física, Universidad de Sevilla, Apdo. 1065, E-41080 Sevilla, Spain.

I. INTRODUCTION

In general terms, the study of reactions which transfer two neutrons to or from a nucleus continues to be important for at least two reasons. The first reason is that there are still few examples where a detailed, realistic, calculation of the reaction rates is successful in describing an extensive set of experimental data both in magnitude and in form. The low energy of the triton beams available so far meant that the simplest reaction to study, $A(t,p)B$, was likely to go via a multistep reaction mechanism which was difficult to model. For example, two forms of two-step mechanisms can be important. In one, the two neutrons are transferred sequentially to the target nucleus while in the other the two neutrons are transferred simultaneously to the target and the target is inelastically excited before the transfer or the residual nucleus is inelastically deexcited after the transfer. It is difficult to

get a realistic, consistent, shell-model description of the states involved and their coupling during the reaction. Also, until recently, the time required for the calculation of, and the addition of, even the one- and the two-step reaction mechanisms using realistic wave functions was beyond the computing power available. Simplified calculations for (t,p) reactions assuming the reaction was the direct transfer of a pair of correlated (s-state) neutrons, underpredicted the observed cross sections by a factor of 2 or 3. It was suggested that the use of the full triton wave function in the calculation [1], or the inclusion of at least the two-step mechanisms [2] would rectify the main failings in the reaction calculation. The results of the most extensive investigation to date, that of the $^{208}Pb(p,t)^{206}Pb$ reaction using 22 MeV polarized protons [3], suggest that for accurate prediction of the data both the above refinements should be included in the calculation along with coupling to excited states in the intermediate channel during the sequential transfer. (Reference [3] also serves as a good introduction to the relevant publications.)

Igarishi, Kubo, and Yagi [3] show predictions of the energy dependence of the one-step and the two-step partial cross sections for transitions to a natural parity state of Pb. It seems curious that the ratio of one-step to two-step cross sections is predicted to show little change for incident proton energies from 20 to 80 MeV. For higher incident energies, there is less time for more complicated reaction processes to occur and it was expected that the calculations could be simpler but still realistic. However, the triton energies needed and the angular range that could be predicted remained to be investigated.

The second reason why the study of two-neutron transfer reactions is important is the older one, that it gives information about two-neutron correlations in the nucleus. It is now clear that even when studying the relative values of the spectroscopic factors for states in a single nucleus, the empirically determined values can be misleading if the varying amounts of the multistep contributions are not correctly removed during the analysis. As emphasized by Pinkston and Satchler [4], the one-step and the two-step contributions to the cross section tend to be very similar in shape and hence are very difficult to separate without prior knowledge of many spectroscopic amplitudes. At the highest incident triton energies used previously (20 MeV) it is plausible that the ratio of two-step to one-step cross sections is 3 or 4 for an allowed transition. Because of the reduced interaction time, it is expected that this ratio will fall if the triton energy is increased and it may be that with 40 MeV tritons incident the one-step (or direct) mechanism will give the bulk of the cross section over part of the angular distribution. If this is so, the extraction of reliable spectroscopic information from the data would be greatly simplified. Other more complex mechanisms would be even less likely to contribute significantly. Originally we believed that in the reaction chosen for study, $^{40}Ca(t,p)^{42}Ca$, the low lying states of the Ca nuclei were well understood. That is, their wave functions could be calculated accurately with the shell model, a large basis set, and tabulated interactions. This work would be a test of the calculation of reaction mechanisms. This idea was also basic to the work on the Ca isotopes reported by Bayman [5] and by Feng and Valeries [6], who calculated the expected cross sections using a full finite-range formalism and the Tang-Herndon form for the triton wave function.

On the following pages is the report of an experiment to find if the (t,p) reaction using the maximum beam energy available at the Nuclear Structure Facility, Daresbury (40 MeV) is recognizably a more direct reaction than when using lower energy triton beams. The variation of the cross sections with energy was measured and the data was analyzed to find if the one- and two-step contributions varied with energy as predicted. Transitions to excited states were measured and analyzed as well as elastic and inelastic scattering and one nucleon transfer reaction rates.

Because of the large positive Q value for a (t,p) reaction, transitions to the low-lying states of the residual nucleus could be cleanly separated from other processes. Most of the lower energy protons and deuterons came from triton breakup after compound nucleus formation but the spectra were not studied carefully. Extra care was taken, however, to ensure that accurate absolute cross sections were obtained as the shapes of the angular distributions were not expected to have much dependence on any of the several underlying reaction mechanisms.

To ensure that the reaction mechanism was correctly modeled, the relevant measured data had to be correctly predicted starting from realistic wave functions for ^{40}Ca, ^{41}Ca, and ^{42}Ca; and using self-consistent shell model calculations to predict the signs of the amplitudes added together in the final coherent sum. In theory, almost any reaction mechanism could be calculated using the CRC code used in the analysis. In practice, the calculations made in the analysis were CCBA calculations as this enabled the easy incorporation of measured values in the *light ion* convention used in optical model analyses. In particular, the potentials derived by England *et al.* [7] in an extensive analysis of new triton scattering data could be used immediately.

In some preliminary calculations, the one-step reaction rates were calculated in the prior-post system with the (t,p) overlap integral calculated using the full triton wave function from solving the Fadeev equations [8]. Although the results from such a model (with direct transfer only), were a reasonable prediction of the ground-state angular distribution, and thus supported the contention of Nagarajan *et al.* [9], it was clear that the neutron, sequential-transfer rates would be at least as large and, when added to the direct-transfer rates, moved these predictions away from the measured rates. The effect of including two-step processes via excited states of the target, the intermediate, or the residual nuclei was unknown.

II. THE EXPERIMENT

The reaction rates for the formation of the ground and first four excited states of ^{42}Ca were measured for tritons incident on ^{40}Ca targets at energies of 28, 33, and 37.3 MeV. Given the high quality tritium beam accelerated by the Nuclear Structure Facility at Daresbury, the measurement and the extraction of the $^{40}Ca(t,p)^{42}Ca$ and related cross sections was straightforward and will not be described in detail here. A full description of the experiment has been given by Becha [10]. Salient points in the experiment plan were that an energy resolution of better than 150 keV was required to separate the products of reactions to the different excited states of

^{42}Ca, that the cross sections are small, and that the protons produced were relatively energetic (the Q value for the ground-state reaction is $+11.3$ MeV).

The protons were detected in six, cooled Si detector telescopes, each consisting of three detectors stacked close together behind a 3 or a 4 mm diameter circular aperture. The range of the protons of interest varied from 8 to 14 mm of silicon and the telescopes were either an 0.5 mm detector followed by two 5 mm ones or two 5 mm detectors and a 3 mm one. Preliminary measurements showed that acceptable resolution was obtained if detector signals were summed after digitization, and that the loss of counts because of scattering out of the active detector regions was small. The electronics were also arranged to record simultaneously the (t,t') and (t,d) reaction data either, at the lower energies, by using an analog particle identification system to sort the events online or, at the highest energy, by storing the detector signals from longer range particles and later using the energy loss recorded for each detector to identify the particle and hence sort the events. When they were determined, the cross sections for triton elastic scattering agreed with those given by England *et al.* [7].

One unusual aspect was the need for very pure ^{40}Ca target foils and the need to find the absolute areal density since failure to do so was a likely source of systematic error in the cross sections. Also the foils became very fragile if oxidized. The thickness of the self-supporting Ca foil used, about $0.5\ \mathrm{mg\ cm^{-2}}$, was too thick to prepare conveniently by vacuum evaporation. The following method for rolling a target foil was developed. Pure Ca metal was prepared by reducing $CaCO_3$ in vacuum on a tantalum strip heater. The Ca metal was taken out of the vacuum into an enclosure filled with a carefully dried atmosphere of pure argon gas. Once there, foils were rolled with the Ca between stainless steel strips. Finally, in the same enclosure, the Ca foils were cut up and mounted on the target holders. These were then placed in a transfer vessel which was immediately evacuated. Later the targets were transferred under vacuum to the target chamber. Even after transfer and several days in the target chamber, the foils remained clear and ductile and no features from the ^{16}O$(t,p)^{18}$O reaction, or from reactions with other Ca isotopes, were seen in the spectra.

To determine the areal density of the target, square pieces of the targets were cut out after the experiment and the area of the pieces carefully measured. The mass of Ca in the pieces was determined by a standard process based on atomic absorption spectroscopy. In this, a suitable solution was made up containing the dissolved piece of foil and the change in the absorption of characteristic Ca lines was measured as the solution was added to an intervening flame. The apparatus was calibrated by comparisons with added standard solutions of similar concentration. Given the mass of Ca and the area of the piece, the areal density was calculated and used when finding the cross section assuming that the target thickness was very uniform. The errors quoted with the cross sections ($\pm 5\%$) are partly from the uncertainty in the determination of the areal density but include a possible systematic error ($\pm 4\%$) from target nonuniformity.

A sample spectrum of protons from the (t,p) reactions is shown in Fig. 1. Protons from reactions with more energy loss were cut off by the coincidence requirements for signals

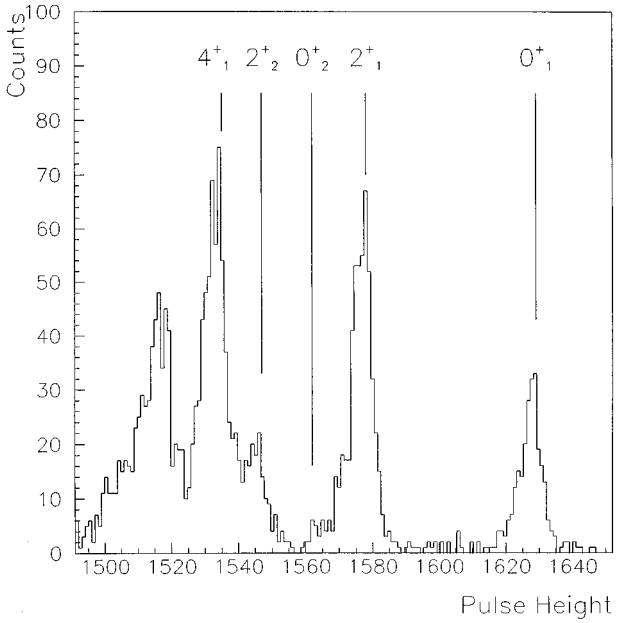

FIG. 1. A sample spectrum of the highest energy ($\simeq 50$ MeV) protons from the ^{40}Ca$(t,p)^{42}$Ca reaction with 37.3 MeV incident energy. The lines added indicate, from right to left, peaks corresponding to transitions to the five lowest energy states in ^{42}Ca. That is to the 0^+_1 (ground), 2^+_1 (1.5246 MeV), 0^+_2 (1.8373 MeV), 2^+_2 (2.4236 MeV), and 4^+_1 (2.7523 MeV) states of ^{42}Ca, respectively.

to be stored but the remainder of the spectrum is known to be dominated by the yields of protons from direct triton breakup and proton emission after compound nucleus formation. The width of the peaks in the proton spectra was not as narrow as expected after a preliminary calculation. Since the usual factors affecting the peak width were well known, and stability of the electronics was continually monitored by test pulses and found to be as expected, it was concluded that small differences in the paths of the detected particles had led to differences in the energy loss in the many dead layers of the stacked detectors. There was some overlap of the peaks of interest, and during the data reduction a simultaneous fit of six Gaussian shaped peaks was made to the relevant part of the spectrum. The area of the peaks was then calculated with the parameters from the fit.

The results for all the angular distributions extracted from the spectra are in a Birmingham Physics Department Internal Report [11] but a large selection of them are plotted in the figures in this paper (see also Ref. [10]). The uncertainty in the measured values is indicated in the figures when it is greater than the size of the symbols. Figure 2 shows that there is structure in the angular distributions, particularly for transitions to the ground state of ^{42}Ca, and that there is a clear energy dependence of that structure, particularly for forward angles.

III. ANALYSIS AND DISCUSSION

As indicated in the introduction, it was not the aim of this work to test new theory but rather to determine empirically if the time for reactions with 40 MeV tritons was sufficiently short that parts of the angular distribution arose almost entirely from direct, two-nucleon transfer. Accordingly the

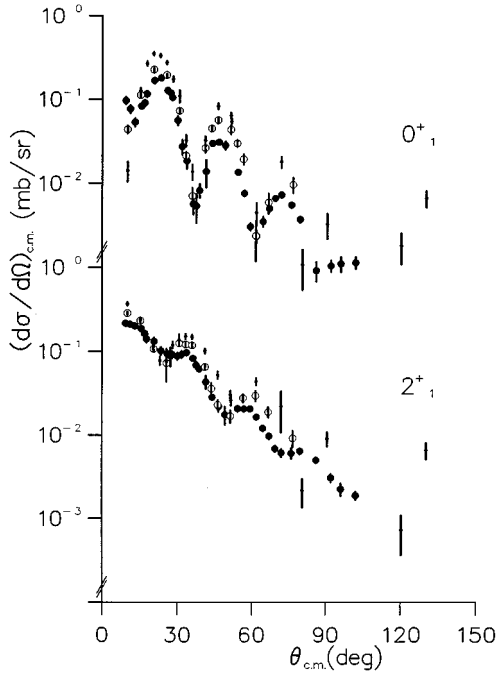

FIG. 2. The measured energy dependence of the differential cross section for the ^{40}Ca(t,p)^{42}Ca reaction to the ground state and first excited state of ^{42}Ca. Values of the differential cross section at 28, 33, and 37.3 MeV incident energy are shown as dots, open circles, and closed circles, respectively.

theory (see, for example, Ref. [12]) is assumed and only the choice of what to calculate and the parameters used are reported. For reference, the low lying and most relevant states of ^{40}Ca, ^{41}Ca, and ^{42}Ca are shown in Fig. 3 and states which are coupled to each other in the one-way DWBA calculations are also indicated there. The energy scale included in the figure shows the relative energies of the excited states but the figure is not drawn so that the correct Q values for the reactions are also shown. Each calculation was repeated using the three incident triton energies 28, 33, and 37.3 MeV to allow direct comparison of the results of calculation with the measured data. A more detailed discussion can be found in Ref. [10].

A. Calculations

The main (standard) reaction calculations were made with the full finite-range code FRESCO [13] and restricted to (one-way coupling) distorted-wave Born approximation (DWBA). This allowed the use of unmodified optical model potentials from the literature for the calculation of the distorted waves. Calculations of one-neutron transfer reaction rates used the post coordinate system so that the usual light-ion assumption that the remnant term is zero was likely to be true. This then required the nonorthogonality correction term to be included in the calculation for sequential neutron transfers. The values of the parameters of the optical-model potentials used are tabulated in Table I where for convenience, the values used in various calculations have been listed together. For the ^{42}Ca+p channel, suitable scattering data had been measured at the three energies of interest [14] and fitted potentials were selected with J_R=365 MeV fm^3. For the ^{41}Ca+d channel, one potential set was calculated using the formula given by Daehnick *et al.* [15], and the other two [16,17] were selected with the assumption that the ^{40}Ca+d potentials are the best available at these energies. Finally for the ^{40}Ca+t channel, the same potential, from a fit to 33 MeV scattering data [7], was used for all three incident triton energies but the one used must be chosen from the three equivalent potentials reported. Results from the simple folding model suggest that

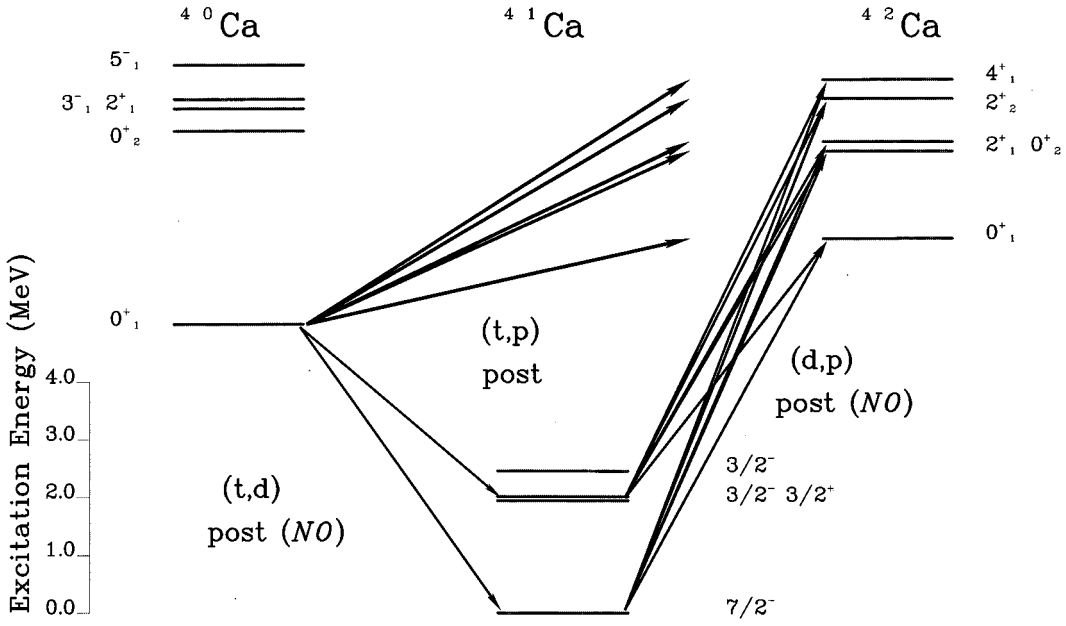

FIG. 3. The low-lying states of ^{40}Ca, ^{41}Ca, and ^{42}Ca. The coupling of states in the ''standard'' CCBA calculations is indicated by the arrows. In the transfer calculations, all combinations of the states indicated by arrows were included, assuming transitions from left to right in the figure. post (NO) indicates that these calculations were made using the post (reaction) coordinate system with the nonorthogonality correction included.

TABLE I. Values of the parameters in the optical model potentials for the three channels used in the calculation of the distorted waves. For all sets, potentials are in MeV, distances in fm, and $r_c = 1.3$ fm. J_R, the real volume integral/interacting pair is in MeV/fm^3.

Potential	System	Energy	V_R	r_R	a_R	W_D	W_V	r_I	a_I	V_{SO}	r_{SO}	a_{SO}	J_R	Ref.
T1	^{40}Ca+t	33.0	152.33	0.980	0.870	16.15		1.341	0.786	3.165	0.786	0.150	332	[7]
T2	^{40}Ca+t	33.0	201.21	1.040	0.764	18.11		1.200	0.879	4.680	1.064	0.197	458	[7]
T3	^{40}Ca+t	33.0	276.71	1.020	0.726	20.75		1.106	0.924	5.567	1.113	0.166	583	[7]
D1	^{40}Ca+d	30.0	93.00	1.130	0.800	10.23		1.390	0.750	5.070	0.900	0.560	390	[16]
D2	^{40}Ca+d	34.4	95.44	1.075	0.804	11.81		1.340	0.764	6.310	1.075	0.804	365	[17]
D3	^{41}Ca+d	39.4	83.36	1.170	0.776	11.32	1.90	1.325	0.740	6.310	1.170	0.776	380	[15]
P1	^{42}Ca+p	40.0	42.98	1.152	0.758	0.435	5.08	1.511	0.460	6.120	0.914	0.759	372	[14]
P2	^{42}Ca+p	45.0	42.84	1.146	0.758	1.520	5.06	1.615	0.414	5.600	1.005	0.711	367	[14]
P3	^{42}Ca+p	48.4	40.34	1.168	0.722	1.297	5.75	1.496	0.586	5.610	0.980	0.790	362	[14]
T4	^{48}Ca+t	33.0	134.88	1.080	0.828	17.14		1.310	0.741	3.210	1.083	0.174	361	[7]
D4	^{49}Ca+d	34.4	95.59	1.087	0.800	11.89		1.280	0.771	7.37	1.287	0.700	386	[17]
P4	^{50}Ca+p	47.8	44.85	1.160	0.750	1.140	7.82	1.370	0.63	6.04	1.064	0.735	386	[18]

the potential with $J_R = 350$ MeV fm^3 would be the physically real one. However, the results from calculations using each of the three equivalent ^{40}Ca+t potentials were investigated.

Two types of overlap integrals (or form factors) must be evaluated. These terms are often called the target overlap integral; and the light-ion or potential overlap integral which contains an interaction potential in the post coordinate system. In that case the potential is that between the final light-ion and the transferred nucleon or nucleons. When the light-ion or potential overlap integrals were calculated, the first requirement was the use of wave functions with the correct asymptotic form. A simplified model was used for the triton and for the deuteron with each represented by only one state with no internal angular momentum. In the neutron sequential transfer calculations a Hulthen form [19] was used for the radial part of the deuteron and the triton wave functions. Following the work of Hering *et al.* [20] we used $\alpha = 0.446$ fm^{-1}, $\beta = 1.36$ fm^{-1} in calculations of the (t,d) differential cross sections and $\alpha = 0.231$ fm^{-1}, $\beta = 1.36$ fm^{-1} in calculations of the (d,p) differential cross sections.

In principle, when evaluating the integrals in the two-neutron direct transfer calculations the Tang-Herndon form was used for the radial part of the triton wave function. A numerical form of the overlap integral, calculated with the above wave function including the hardcore correction, was available from the code FRUCK2 [21] but unfortunately the tabulation is not compatible with the integration sequence in the code FRESCO. Hence in practice two calculations of the (t,p) reaction rate were performed initially and the results compared. One calculation used the code FRUCK2 with the light-ion overlap integral calculated assuming the Tang-Herndon form for the triton wave function. The other calculation used the code FRESCO with all parameters the same as in the first calculation except that the triton wave function in the light-ion integral was calculated using the Woods-Saxon, half-separation energy, potential prescription. It was found that the two calculated angular distributions had very similar shapes but differed in magnitude and it was concluded that the results of a calculation using the code FRESCO and Tang-Herndon form for the triton wave function in the light ion integral would be very close to those calculated using the Woods-Saxon potential prescription, if the calculated (t,p) cross section results in the latter case were multiplied by a factor of 1.5. Thus in the calculations reported, the light-ion integral for direct, two-nucleon transfer was calculated using the Woods-Saxon, half-separation energy prescription and resulting cross sections multiplied by 1.5 to give the results presented.

To evaluate the target overlap integrals, shell-model calculations of the properties of the states indicated in Fig. 3 were made first using the code OXBASH5 [22]. Some calculations were made with the parameter values given by Federman and Pittel [23] which assumes that only nucleons in the $d_{3/2}$ and $f_{7/2}$ shells are active. From other experiments [24] this seems unlikely, particularly for the excited states of ^{42}Ca. The results will not be reported except for the comment that the values of the total reaction rates calculated were not very different from the ones reported below. Shell-model calculations using the same basis set and effective interactions as Warburton *et al.* [25] were made for all the relevant Ca nuclei and the resulting overlap amplitudes are shown in Tables II and III. These were then used in the final calculations using the code FRESCO. To ensure that the relative phases of the amplitudes are significant, care was taken to use the same basis and effective interactions for all calculations. Because of the limits to the computer available to us, the number of particles allowed in the subshells used were $1d_{3/2}$ (4 to 8), $1f_{7/2}$ (0 to 4), $2p_{3/2}$ (0 to 2). The particle could be a proton or a neutron.

In the calculations using FRESCO, the radial integrals in the target overlap section were computed using apparently much simpler wave functions. For one-neutron transfers these were generated so as to bind the neutron with the known separation energy in a single particle orbital in a Woods-Saxon potential, thus ensuring the correct asymptotic form. For the two-neutron transfer, the transferred neutrons were assumed to be in a relative $l = 0$, $s = 0$ state and the half separation energy, well-depth procedure was used when constructing the radial wave functions. In this case, that meant that the wave function described two neutrons each of which was bound to a ^{40}Ca core in a state whose binding energy was half the real two-neutron separation energy of such a simple state in ^{42}Ca. The Woods-Saxons well was a real central potential with $R = 1.25A^{1/3}$ fm, $a = 0.65$ fm, plus a

TABLE II. The spectroscopic amplitudes for the overlap integrals in one-nucleon transfer between the light Ca isotopes calculated with the shell-model code as described in the text.

Initial state		Final state		Spectroscopic amplitude		
Nucleus	J,T	Nucleus	J,T	$1d_{3/2}$	$1f_{7/2}$	$2p_{3/2}$
^{40}Ca	$0^+_1,0$	^{41}Ca	$\frac{7}{2}^-_1,\frac{1}{2}$		0.980	
^{40}Ca	$0^+_1,0$	^{41}Ca	$\frac{3}{2}^-_1,\frac{1}{2}$			0.981
^{40}Ca	$2^+_1,0$	^{41}Ca	$\frac{7}{2}^-_1,\frac{1}{2}$			
^{40}Ca	$2^+_1,0$	^{41}Ca	$\frac{3}{2}^-_1,\frac{1}{2}$		0.008	0.010
^{40}Ca	$3^-_1,0$	^{41}Ca	$\frac{7}{2}^-_1,\frac{1}{2}$	0.646		
^{40}Ca	$3^-_1,0$	^{41}Ca	$\frac{3}{2}^-_1,\frac{1}{2}$	0.013		
^{41}Ca	$\frac{7}{2}^-_1,\frac{1}{2}$	^{42}Ca	$0^+_1,1$		−1.404	
^{41}Ca	$\frac{7}{2}^-_1,\frac{1}{2}$	^{42}Ca	$2^+_1,1$		−1.385	−0.124
^{41}Ca	$\frac{7}{2}^-_1,\frac{1}{2}$	^{42}Ca	$0^+_2,1$		0.030	
^{41}Ca	$\frac{7}{2}^-_1,\frac{1}{2}$	^{42}Ca	$2^+_2,1$		−0.181	0.977
^{41}Ca	$\frac{7}{2}^-_1,\frac{1}{2}$	^{42}Ca	$4^+_1,1$		1.392	0.090
^{41}Ca	$\frac{3}{2}^-_1,\frac{1}{2}$	^{42}Ca	$0^+_1,1$			−0.235
^{41}Ca	$\frac{3}{2}^-_1,\frac{1}{2}$	^{42}Ca	$2^+_1,1$		−0.124	−0.068
^{41}Ca	$\frac{3}{2}^-_1,\frac{1}{2}$	^{42}Ca	$0^+_2,1$			−0.034
^{41}Ca	$\frac{3}{2}^-_1,\frac{1}{2}$	^{42}Ca	$2^+_2,1$		0.977	0.164
^{41}Ca	$\frac{3}{2}^-_1,\frac{1}{2}$	^{42}Ca	$4^+_1,1$		0.089	

TABLE III. The spectroscopic amplitudes for the overlap integrals in two-nucleon transfer from ^{40}Ca calculated with the shell-model code as described in the text.

Init. ^{40}Ca	Final ^{42}Ca	Transf.	Spectroscopic amplitude					
J,T	J,T	J	$1d^2_{3/2}$	$1f^2_{7/2}$	$1f_{7/2}1d_{3/2}$	$2p_{3/2}1d_{3/2}$	$2p_{3/2}1f_{7/2}$	$2p^2_{3/2}$
$0^+_1,0$	$0^+_1,1$	0	0.210	−0.975				−0.165
$0^+_1,0$	$2^+_1,1$	2	0.052	−0.960			−0.121	−0.047
$0^+_1,0$	$0^+_2,1$	0	0.004	0.024				−0.024
$0^+_1,0$	$2^+_2,1$	2	−0.007	−0.126			0.956	0.113
$0^+_1,0$	$4^+_1,1$	4	0.965					0.087
$2^+_1,0$	$0^+_1,1$	2	−0.483	0.141			−0.002	0.001
$2^+_1,0$	$2^+_1,1$	0	0.516	−0.056				−0.020
$2^+_1,0$	$2^+_1,1$	2	−0.001	−0.051			−0.005	−0.001
$2^+_1,0$	$2^+_1,1$	4	0.072				−0.005	
$2^+_1,0$	$0^+_2,1$	2	−0.103	−0.383			−0.063	−0.019
$2^+_1,0$	$2^+_2,1$	0	0.027	0.005				0.005
$2^+_1,0$	$2^+_2,1$	2	0.016	−0.001			−0.028	0.003
$2^+_1,0$	$2^+_2,1$	4		0.015			0.002	
$2^+_1,0$	$4^+_1,1$	2		−0.051			0.003	0.001
$2^+_1,0$	$4^+_1,1$	4		0.007			0.003	
$2^+_1,0$	$4^+_1,1$	6		−0.043				
$3^-_1,0$	$0^+_1,1$	3			0.897	−0.001		
$3^-_1,0$	$2^+_1,1$	1				0.058		
$3^-_1,0$	$2^+_1,1$	3			0.570	0.019		
$3^-_1,0$	$2^+_1,1$	5			0.118			
$3^-_1,0$	$0^+_2,1$	3			0.029	−0.008		
$3^-_1,0$	$2^+_2,1$	1				−0.454		
$3^-_1,0$	$2^+_2,1$	3			0.071	−0.154		
$3^-_1,0$	$2^+_2,1$	5			0.004			
$3^-_1,0$	$4^+_1,1$	1				0.036		
$3^-_1,0$	$4^+_1,1$	3			0.080	−0.042		
$3^-_1,0$	$4^+_1,1$	5			−0.413			

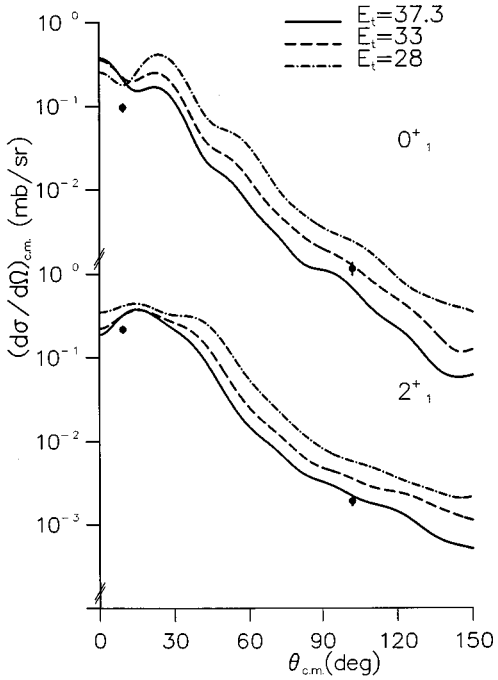

FIG. 4. The predicted energy dependence of the differential cross section for the ^{40}Ca$(t,p)^{42}$Ca reaction to the ground state and first excited state of ^{42}Ca. Values for the differential cross section at 28, 33, and 37.3 MeV incident energy are shown by dot-dashed, dashed, and solid lines, respectively.

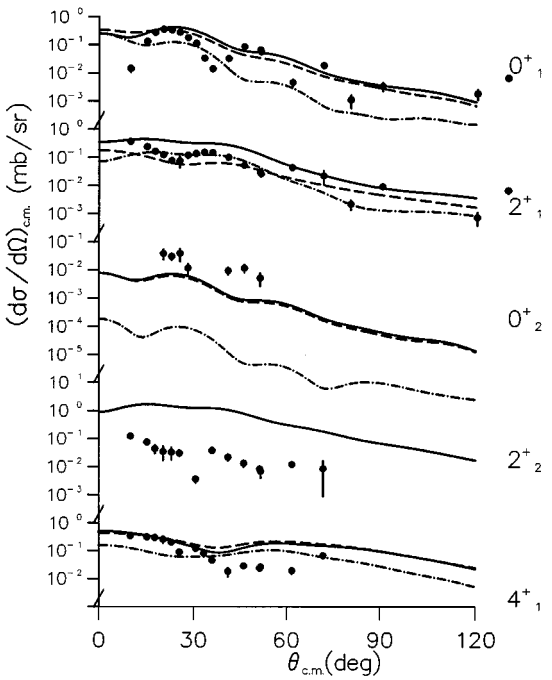

FIG. 5. A comparison of the measured differential cross sections with the predictions made using the code FRESCO as described in the text (continuous lines), for transitions to states in ^{42}Ca and 28 MeV incident triton energy. Also shown are the calculated one-step (dot-dashed lines) and two-step (dashed lines) partial cross sections for transitions to several states.

Thomas form, spin-orbit potential with a depth of 4 MeV, radius of 1.25 fm, and diffuseness of 0.6 fm. Again, the aim was to use wave functions with the correct asymptotic form.

Calculations were made using the Born approximation and assuming that all the one-step transfers were from the ground state of ^{40}Ca and all the two-step transfers were via the ground and first excited state of ^{41}Ca. No attempt was made to adjust the overlap amplitudes predicted from shell-model wave functions so as to predict the observed ^{40}Ca$(t,d)^{41}$Ca reaction rates.

B. Comparison with data

An important feature of this experiment is the measurement of the reaction rates for almost all the open scattering and reaction channels so that many features predicted with our model can be immediately verified. Although it is included to make another point, Fig. 11 shows an example of the agreement of the predictions and the data for single neutron transfer. At each energy, the predictions from a single calculation were in similar agreement with the measurements for all the scattering and one nucleon transfer channels including the $(t,{}^3\mathrm{He})$, charge-exchange one. (More examples can be found in Pinder *et al.* [26])

Figure 4, which is constructed to allow easy comparison with Fig. 2, shows the predictions for the ^{40}Ca$(t,p)^{42}$Ca reaction rates calculated using the code FRESCO as outlined in the previous section. Notice the rapid variation with energy of the calculated ground state angular distribution near 0°. Figure 5 shows a comparison of the predictions and the measured data for transitions to different final states in ^{42}Ca for 28 MeV incident triton energy. After the preliminary calculations described above there are no adjustable parameters to fit the predictions to the data. Hence it is encouraging that the calculated angular distributions have the right magnitude and slope in most cases, with oscillations about the trend whose amplitude falls rapidly as the excitation of the final state increases. It is noted that a better prediction of the angular distribution of transitions to the 2^+_2 state is made if in the calculations, our 2^+_2 amplitudes are replaced by the 2^+_1 amplitudes. The success of the calculation in predicting the magnitude and overall shape of the data for many processes means that some conclusions can be drawn from this study but it cannot be said that the results of calculation predict the data with convincing detail.

The ratio of the one-step to the two-step cross sections, the major components of the total cross section, was found to be about unity and fell slowly with incident energy. Figure 6 shows the partial cross sections of the one- and the two-step neutron transfer reactions for transitions to the 4^+ state and their predicted energy dependence. Consideration of the results in Appendix A of Ref. [3] suggests that the predicted, two-step transfer, cross section might be reduced by a factor less than 2 if a more realistic triton wave function than the Tang-Herndon one was used, but it remains clear that the two-step process must be calculated in detail before reliable spectroscopic factors can be extracted from data taken with similar incident energies. No region of the angular distributions is dominated by direct transfers. This was predicted to occur at forward angles for transfers to the 2^+_2 state with 37.3 MeV incident energy. It is clear, however, that the reaction rates to this state are not predicted with our Shell model overlaps and no conclusions can be drawn in this case.

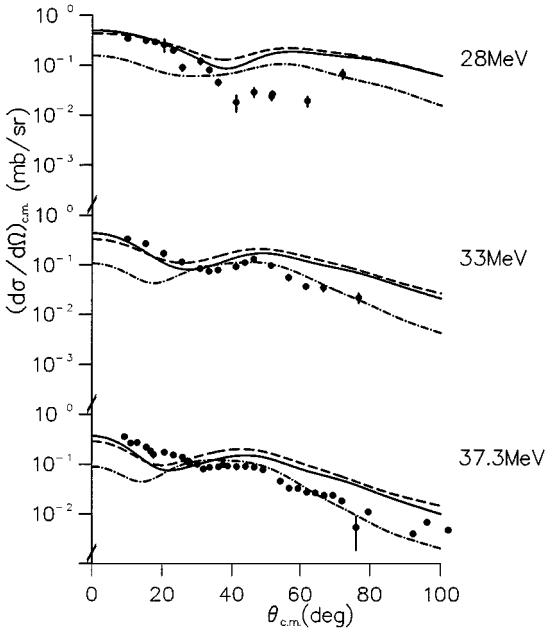

FIG. 6. The data and the energy dependence of the predicted cross sections for transitions to the 4_1^+ state. At each energy, the one-step (direct) partial cross section is shown by the dot-dashed line, the two-step (sequential) contribution by the dashed line, and the coherent sum of both contributions by the solid line.

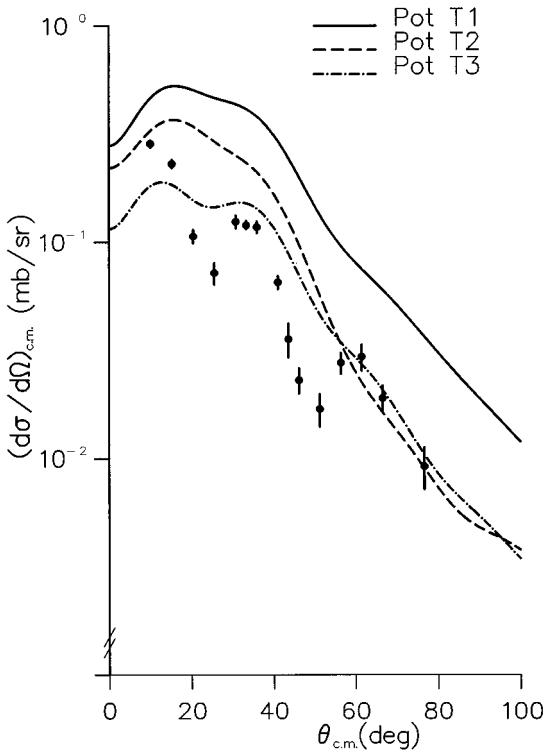

FIG. 7. The variation of the predicted cross section of the 2_1^+ state with optical-model set used in calculating the ingoing distorted waves. The data shown and the calculations are for 33 MeV incident triton energy.

In the Introduction, it was noted that the results of previous work on (t,p) reactions with 7 MeV/nucleon incident energy suggest that the ratio of two-step to one-step partial cross sections is 3 or 4 for allowed transitions. From this work we conclude that the ratio is $\simeq 1$ with 14 MeV/nucleon incident energy. The interaction time falls with increasing incident energy and with this the amount of more complicated reaction mechanisms should be suppressed more than the amount of direct two-nucleon transfer. It is concluded that at least 30 MeV/nucleon incident energy is needed before it is reasonable to use a simple analysis to extract information about two-nucleon correlations in nuclei from measurements on (t,p) reactions.

IV. FURTHER ANALYSIS

The cross section predicted is relatively sensitive to the optical-model potential set chosen when calculating the distorted waves for the ^{40}Ca$+t$ channel and this is a problem when the magnitude of the cross sections is used to extract properties of the nuclear states. An example of the effect is shown in Fig. 7. Because of the uncertain *dynamic* potentials that must be added to the calculated, double-folding potentials for a realistic description, such estimates are not definitive and there seems to us to be no good reason in this case for choosing either the potential set with $J_R = 460$ MeV fm^3 or the set with $J_R = 580$ MeV fm^3.

Some further calculations were made to see if fitting inelastic scattering data, or allowing further excitations of the intermediate nuclei, could lead to the selection of the true potential. The problem was not resolved when coupling to inelastic states was explicitly included in the CCBA calculations as follows. Macroscopic models of the initial and final systems as deformed rotors were used to calculate the internal couplings between states and the amplitudes for transitions between nuclei were taken from the Shell model calculations already reported. In discussing the macroscopic model, the notation detailed by Tamura [27] is used.

Relevant deformation parameters were determined by fitting the results of a full coupled-channels calculation to the data for ^{40}Ca$(t,t')^{40}$Ca* scattering [11]. The lowest lying 3^- state was modeled as a 1 $\hbar\omega$, octupole vibrational state and β_{03} found to be 0.19 if the optical model radii detailed in Table I are used. (The deformation length βR is more reliably determined.) The 2_1^+ state was modeled as a 2 $\hbar\omega$, octupole vibrational state and β_{32} (two step) found to be 0.134, β'_{02} (one step) to be 0.033. The 5^- state was modeled as a quadrupole-octupole vibrational state and the β_{35} (two step) and β_{05} (one step) both found to be 0.087. Further deformation parameters were determined from fitting the results reported by Mani *et al.* [28] for ^{42}Ca$(p,p')^{42}$Ca* scattering with $E_p = 49.75$ MeV. The optical model parameters used to describe the elastic scattering are the set P3 in Table I and only the states of interest here are discussed. These states were modeled as quadrupole vibrational states with the 2_1^+ state the 1 $\hbar\omega$ type and the 0_2^+, 2_2^+, 4_1^+ states the 2 $\hbar\omega$ triplet. The deformation parameters determined and the values found were $\beta_{02} = \beta'^2_{00} = 0.103$, $\beta''_{00} = 0.02$, $\beta_{20} = 0.053$, $\beta''_{02} = 0.04$, and $\beta''_{04} = 0.079$. To correct for the collective couplings being treated explicitly in the coupled-channels calculation, the depths of the imaginary optical potentials were reduced so that $W_V = 5.18$ MeV and $W_D = 1.17$ MeV.

As illustrated in Fig. 8, the extra calculation improves the prediction of the (t,p) reaction rates a little but not by the

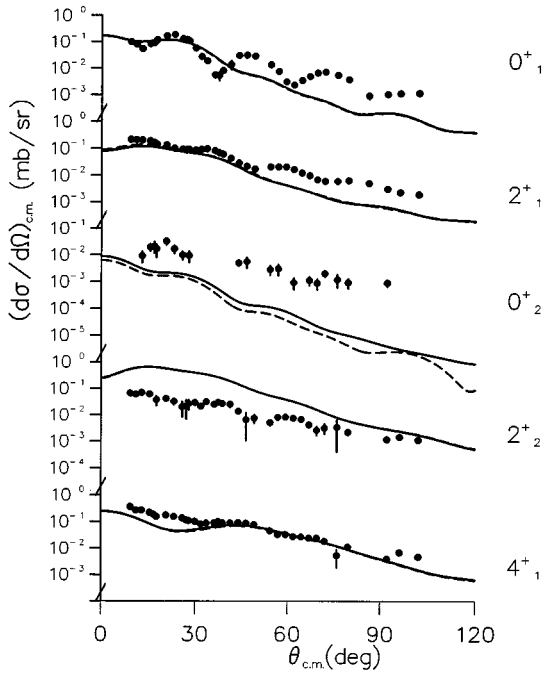

FIG. 8. A comparison of the measured cross sections to the five lowest energy states in ^{42}Ca with 37.3 MeV incident energy, with predictions calculated with (solid lines), or without (dashed lines), inelastic couplings to excited states in the target and residual nuclei.

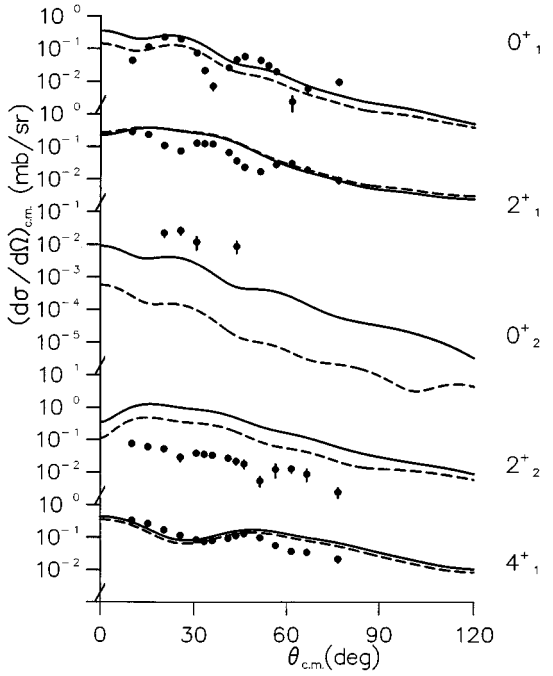

FIG. 9. A comparison of the measured cross sections to the five lowest energy states in ^{42}Ca with 33 MeV incident energy, with predictions calculated with (solid lines), or without (dashed lines) including transitions through the first $\frac{3}{2}^-$ state of the intermediate nucleus ^{41}Ca.

amount required to start selecting between the ambiguous optical potentials. On average, the same must be said about the inclusion in the calculation of transfers via the first excited state of ^{41}Ca. This was expected to be a significant intermediate state. A sample of the results of leaving out such transfers from the standard calculation is shown in Fig. 9. In particular, there is no change in the prediction of the structure in the angular distribution for transitions to the ground state. Given the above results, it is not surprising that it was found that comparison of the predictions with the data did not allow the sensible selection of one of the possible $^{40}\mathrm{Ca}+t$ optical potentials. It is disappointing that, in spite of predicting so much data, no way was found to remove sensibly the ambiguity in selecting optical model potentials and hence to determine spectroscopic amplitudes from such data.

The predictions clearly do not show the structure seen in the angular distributions and this situation is like that found when predicting (t,α) angular distributions. The $^{40}\mathrm{Ca}(t,p)^{42}\mathrm{Ca}$ reaction has a particularly large Q value and it is likely that accurate wave functions in the important overlap region are not being determined by the fits to the elastic and inelastic scattering data. It should also be noted, however, that most of the protons emitted are from triton break up or after compound nucleus formation. Our optical model for these processes is very simple and there is no comparison of the predictions with data.

V. CONCLUSIONS

A large and representative set of data has been assembled showing the results of measurements on most of the possible channels in the $^{40}\mathrm{Ca}+t$ system when incident triton energies are from 9 to 13 MeV/nucleon. (Not all that data comes from the experiments reported above.) The use of solid-state detectors and fast electronic, particle identification seems to have assured that accurate cross sections were obtained over a large range of angles and residual excitation energies.

Careful, extensive, and quantitative calculations using two-nucleon transfer reaction theory and shell-model wave functions for the Ca isotopes were not successful in predicting the (t,p) reaction rates along with those in the other channels. This was particularly true for transitions to the ground state of ^{42}Ca although the cross sections predicted were of the right order of magnitude. It is also apparent that if fitting to data were to be used to extract spectroscopic amplitudes for the light Ca isotopes, the values extracted would be dependent on the choice of one of the ambiguous, optical potential sets determined from the triton elastic scattering data.

ACKNOWLEDGMENTS

We are grateful for the facilities and help made available at the N.S.F. Daresbury Lab.; particularly to R. Darlington and D. Eastman for the preparation of the Ca targets, and to W. Newton for the accurate determination of their Ca content. This work was supported in part by the Science and Engineering Research Council of the United Kingdom.

APPENDIX A: THE $^{48}\mathrm{Ca}(t,p)^{50}\mathrm{Ca}$ REACTION

While great care was taken to ensure the accuracy and validity of the calculations reported in the main text, it is of interest to know if the prediction of other $\mathrm{Ca}(t,p)$ reaction rates has similar failings.

A relatively small amount of data was taken for the

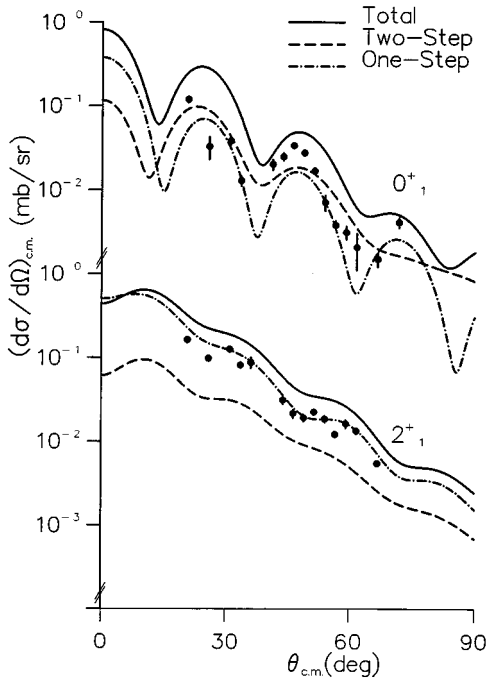

FIG. 10. A comparison of the measured differential cross sections to the two lowest energy states in ^{50}Ca with the predictions made using the code FRESCO as described in Appendix A, and 37.3 MeV incident triton energy, i..e, for transitions to the 0^+_1 (ground) and 2^+_1 (1.03 MeV) states in ^{50}Ca.

^{48}Ca$(t,p)^{50}$Ca reaction with 37.3 MeV incident triton energy and the same experimental setup. In this case the accuracy of the cross sections was mainly limited by a possible systematic error of up to 15% in the estimate of the number of target nuclei. The measured cross sections are shown in Figs. 10 and 11. Also shown in the figures are the results of the same calculations as those described in the main report except for the necessary changes to the constants and the changes to the parameter values described below. The values of the potential parameters used in the distorted wave calculations were changed to the appropriate ones in Table I. New calculations of shell-model amplitudes for use in the calculation of the overlap integrals were made for ^{48}Ca, ^{49}Ca, and ^{50}Ca using the basis set and residual interactions reported by van Hees *et al.* [29]. The calculated values of the resulting spectroscopic amplitudes are shown in Tables IV and V. With these changes, our standard calculation summing the one step transfers from the ground state of ^{48}Ca and the two-step transfers via the ground, $\frac{1}{2}^-$, and $\frac{5}{2}^-$ states of ^{49}Ca gives an acceptable prediction of all the measured cross sections, again, without adjustments to fit the measured ^{48}Ca$(t,d)^{49}$Ca reaction rates.

APPENDIX B: J^π OF THE SECOND EXCITED STATE OF ^{49}Ca

The J^π of the second excited state of ^{49}Ca is predicted to be $\frac{7}{2}^-$ by the shell-model calculation. Such high spin states cannot be reached by direct one-nucleon transfers from the ^{48}Ca shell model state included in the calculation reported above. The $\frac{7}{2}^-$ state could, however, be excited by inelastic excitation of the ^{48}Ca to its 2^+_1 state followed by a direct neutron transfer. To include this channel, the rates for inelastic excitation of ^{48}Ca were calculated from a macroscopic model like that introduced in Sec. IV. In addition to the potentials listed in Table I, this required the deformation pa-

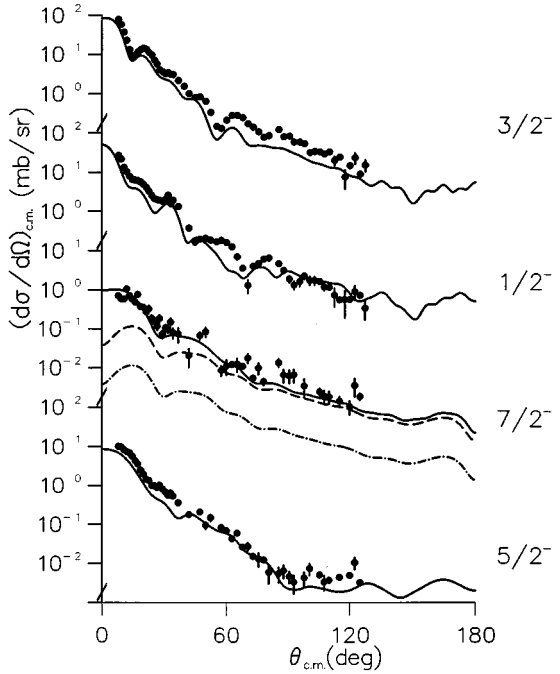

FIG. 11. A comparison of the measured differential cross-sections with the predictions made using the code FRESCO as described in the text (continuous lines), for transitions to the four lowest energy states in ^{49}Ca and 37.3 MeV incident triton energy, i.e., for transitions to the $\frac{3}{2}^-$ (ground), $\frac{1}{2}^-$ (2.022 MeV), $\frac{7}{2}^-$ (3.351 MeV), and $\frac{5}{2}^-$ (3.586 MeV) states in ^{49}Ca. See Appendix B for the meaning of the dashed and the dot-dashed lines.

TABLE IV. The spectroscopic amplitudes for the overlap integrals in two-nucleon transfer from ^{48}Ca calculated with the shell-model code.

Init. ^{48}Ca	Final ^{50}Ca	Transf.	Spectroscopic amplitude					
J,T	J,T	J	$2p^2_{3/2}$	$1f_{5/2}2p_{3/2}$	$1f^2_{5/2}$	$2p_{1/2}2p_{3/2}$	$2p_{1/2}1f_{5/2}$	$2p^2_{1/2}$
0^+_1,4	0^+_1,5	0	−0.965		−0.164			−0.173
0^+_1,4	2^+_1,5	2	−0.949	0.054	−0.044	0.152	−0.068	
0^+_1,4	2^+_2,5	2	−0.152	−0.085	0.056	−0.948	0.124	

TABLE V. The spectroscopic amplitudes for the overlap integrals in one-nucleon transfer between the heavy Ca isotopes calculated with the shell-model code.

Initial state		Final state		Spectroscopic amplitude			
Nucleus	J,T	Nucleus	J,T	$1f_{7/2}$	$2p_{3/2}$	$1f_{5/2}$	$2p_{1/2}$
^{48}Ca	$0_1^+,4$	^{49}Ca	$\frac{3}{2}^-_1,\frac{9}{2}$		−0.973		
^{48}Ca	$0_1^+,4$	^{49}Ca	$\frac{1}{2}^-_1,\frac{9}{2}$				−0.988
^{48}Ca	$0_1^+,4$	^{49}Ca	$\frac{5}{2}^-_1,\frac{9}{2}$			−0.660	
^{48}Ca	$2_1^+,4$	^{49}Ca	$\frac{3}{2}^-_1,\frac{9}{2}$	1.088	−0.082	0.073	0.125
^{48}Ca	$2_1^+,4$	^{49}Ca	$\frac{1}{2}^-_1,\frac{9}{2}$				−0.143
^{48}Ca	$2_1^+,4$	^{49}Ca	$\frac{7}{2}^-_1,\frac{9}{2}$		−0.222	−0.006	
^{48}Ca	$2_1^+,4$	^{49}Ca	$\frac{5}{2}^-_1,\frac{9}{2}$	0.004	−0.678	0.057	0.090
^{49}Ca	$\frac{3}{2}^-_1,\frac{9}{2}$	^{50}Ca	$0_1^+,5$		1.341		
^{49}Ca	$\frac{1}{2}^-_1,\frac{9}{2}$	^{50}Ca	$0_1^+,5$			0.230	
^{49}Ca	$\frac{7}{2}^-_1,\frac{9}{2}$	^{50}Ca	$0_1^+,5$	−2.573			
^{49}Ca	$\frac{5}{2}^-_1,\frac{9}{2}$	^{50}Ca	$0_1^+,5$			0.124	
^{49}Ca	$\frac{3}{2}^-_1,\frac{9}{2}$	^{50}Ca	$2_1^+,5$	−0.127	1.357	0.056	0.153
^{49}Ca	$\frac{1}{2}^-_1,\frac{9}{2}$	^{50}Ca	$2_1^+,5$		−0.145	0.066	
^{49}Ca	$\frac{7}{2}^-_1,\frac{9}{2}$	^{50}Ca	$2_1^+,5$	0.457	−0.088		0.032
^{49}Ca	$\frac{5}{2}^-_1,\frac{9}{2}$	^{50}Ca	$2_1^+,5$	0.791	0.051	0.058	−0.061
^{49}Ca	$\frac{3}{2}^-_1,\frac{9}{2}$	^{50}Ca	$2_2^+,5$	0.110	0.226	−0.082	−0.961
^{49}Ca	$\frac{1}{2}^-_1,\frac{9}{2}$	^{50}Ca	$2_2^+,5$		0.951	−0.124	
^{49}Ca	$\frac{7}{2}^-_1,\frac{9}{2}$	^{50}Ca	$2_2^+,5$	−0.162	−0.020	0.010	
^{49}Ca	$\frac{5}{2}^-_1,\frac{9}{2}$	^{50}Ca	$2_2^+,5$	−0.007	0.083	−0.008	−0.116

rameter β_{02} and the value of 0.13 given by Ogilvie *et al.* [30] was used. Combining these calculated amplitudes with those for the ^{48}Ca(2^+) to ^{49}Ca($\frac{7}{2}^-$) process (see Table V) in a full CCBA calculation gives the rates shown by the dot-dashed line in Fig. 11. Since there are possibly significant defects in the $f-p$ shell model description or in the simple mixing of results from collective and microscopic models, the latter amplitude can reasonably be multiplied by 3. The results of a full calculation using this value are shown by the dashed curve. There is believed to be $1f_{7/2}$ hole admixtures in the low lying states of ^{48}Ca [24] so a direct transfer with amplitude ($\sqrt{S}$) of $\sqrt{0.05}$ was included in the full calculation with the modified two-step amplitude and the results are shown by the continuous line. The forward peaked distribution for the direct $1f_{7/2}$ transfer improves the agreement with the data.

The data clearly does not possess a sufficiently rapid fall with angle to be due to just a $1f_{7/2}$, a $2p_{3/2}$, a $1f_{5/2}$, or a $2p_{1/2}$ transfer. This can be seen by comparison of the angular distribution with those for transitions to the $\frac{3}{2}^-$, $\frac{1}{2}^-$, and $\frac{5}{2}^-$ states. Neither the $\frac{9}{2}^+$ assignment for the second excited state reported by Abegg *et al.* [31], nor the $\frac{5}{2}^+$ assignment reported by Metz *et al.* [32], lead to similar quality prediction of the measurements. It is reassuring that the results of shell-model calculations of low lying levels in ^{49}Ca reported by Martinez-Pinedo *et al.* [33] also give a $\frac{7}{2}^-$ for the second excited state.

[1] M. F. Werby, M. R. Strayer, and M. A. Nagarajan, Phys. Rev. C **21**, 2235 (1980).

[2] N. B. de Takacsy, Nucl. Phys. **A231**, 243 (1970).

[3] M. Igarishi, K. Kubo, and K. Yagi, Phys. Rep. **199**, 1 (1991).

[4] W. T. Pinkston and G. R. Satchler, Nucl. Phys. **A383**, 61 (1982).

[5] B. F. Bayman, Nucl. Phys. **A168**, 1 (1971).

[6] D. H. Feng, R. H. Ibarra, and M. Valeries, Phys. Lett. **46B**, 37 (1973).

[7] J. B. A. England *et al.*, Nucl. Phys. **A475**, 422 (1987).

[8] A. Laverne and C. Gignoux, Nucl. Phys. **A203**, 597 (1973).

[9] M. A. Nagarajan, M. R. Strayer, and M. F. Werby, Phys. Lett. **67B**, 141 (1977).

[10] M. B. Becha, Ph.D. thesis, University of Birmingham, 1991.

[11] C. N. Pinder, Birmingham University Physics Department Internal report, 1997 (unpublished). Results from experiments with 30–40 MeV Tritium beams.

[12] G. R. Satchler, *Direct Nuclear Reactions* (Clarendon, Oxford 1983); see also, N. Austern, *Direct Nuclear Reaction Theories* (Wiley, New York, 1970).

[13] I. J. Thompson, Comput. Phys. Rep. **7**, 167 (1988).

[14] R. H. McCamis *et al.*, Phys. Rev. C **33**, 1624 (1986).

[15] W. W. Daehnick, J. D. Childs, and Z. Vrcelj, Phys. Rev. C **21**, 2253 (1980).

[16] R. Roche *et al.*, Nucl. Phys. **A220**, 381 (1974).

[17] E. Newman, L. C. Becker, B. M. Preedom, and J. C. Hiebert, Nucl. Phys. **A100**, 225 (1967).

[18] F. D. Becchetti and G. W. Greenlees, Phys. Rev. **182**, 1190 (1969).

[19] L. Hulthen and M. Sugawara, in *Handbuch der Physik*, edited by S. Flugge (Springer, Berlin, 1957), p. 1.
[20] W. R. Hering, H. Becker, C. A. Wiedner, and W. J. Thompson, Nucl. Phys. **A151**, 33 (1970).
[21] J. R. Comfort, finite-range DWBA computer code FRUCK2 (extended version of computer code FRUCK, P. D. Kunz, 1980), 1983 (unpublished).
[22] A. Etchegoyen *et al.*, Michigan State University version of the Shell-model computer code OXBASH, Michigan State University-NSCL Report No. 524, 1985 (unpublished).
[23] P. Federman and S. Pittel, Phys. Rev. **186**, 1106 (1969).
[24] H. T. Fortune, J. Phys. Soc. Jpn. **44**, 105 (1978).
[25] E. K. Warburton *et al.*, Phys. Rev. C **34**, 1031 (1986).
[26] C. N. Pinder *et al.*, Nucl. Phys. **A533**, 25 (1991).
[27] T. Tamura, Rev. Mod. Phys. **37**, 679 (1965); T. Tamura, Prog. Theor. Phys. Suppl. Jpn. **37** & **38**, 383 (1966).
[28] G. S. Mani, D. Jacques, and D. T. Jones, Nucl. Phys. **A165**, 384 (1971).
[29] A. G. M. van Hees and P. W. M. Glaudemans, Z. Phys. A **303**, 267 (1981).
[30] C. A. Ogilvie *et al.*, Nucl. Phys. **A456**, 445 (1987).
[31] R. Abegg, J. D. Hutton, and M. E. Williams-Norton, Nucl. Phys. **A303**, 121 (1978).
[32] W. D. Metz, W. D. Callender, and C. K. Bockelman, Phys. Rev. C **12**, 827 (1975).
[33] G. Martinez-Pinedo, A. P. Zuker, A. Poves, and E. Caurier, Phys. Rev. C **55**, 187 (1997).